Some experiments on electron scattering from an atomic lattice

D. G. Kiryan and G. V. Kiryan

Institute of Problems of Mechanical Engineering of RAS
61 Bolshoy Prospect V.O., 199178, Saint-Petersburg, Russia
e-mail: diki.ipme@gmail.com

This paper considers some aspects of the dynamics of material particles (electrons, neutrons) in their interaction with atomic nuclei of the target which is an ordered atomic lattice. In this study, we took into account a number of key factors affecting the particle trajectory, namely the inverse square law (Coulomb's law), physical collisions of both elastic and inelastic character, and also the effect of a velocity decrease accompanied by bremsstrahlung.

Analysis of the obtained results of mathematical modeling of material particles scattering from atomic lattices allowed us to reasonably assert that the particles do not possess wave properties giving rise to interference or diffraction. Here we propose a technique allowing practical demonstration of the absence of wave properties in electrons, as well as in other material bodies.

Keywords: scattering of material particles, de Broglie wave, diffraction, interference, wave-particle duality, photon inertial mass.

1. Introduction

In 1923, Louis de Broglie proposed [1] the hypothesis that material particles, as well as larger material bodies, should exhibit in motion wave properties accessible to observation and recording. As de Broglie has written in his book [2], this assumption was made under the influence of Einstein's article on the photoelectric effect [3]. In that work, to solve the problem, Einstein presented electromagnetic radiation as many independent *light quanta*[1] having mechanical momenta, which were later called photons. Thus, Einstein postulated the concept of wave-particle duality, that is, the duality of a photon that may be a wave or material particle depending on the circumstances.

[1] In German: das Lichtquant

De Broglie reasoned in a similar but mirror-like manner and suggested that a moving material particle should exhibit wave properties and would have its own conventional *pilot wave* with the wavelength defined as

$$\lambda = h/mv \ , \tag{1}$$

where λ is the wavelength; h is the quantum of action or Planck's constant; m is the material particle inertial mass; v is the particle velocity. At the heart of de Broglie's reasoning there is the equality whose essence is appropriately presented in the book by H. Mark and R. Wierl [4] on page 14.

> *Based on the main provisions of the theory of relativity and quantum theory of light, assume that*
>
> $$m_0 c^2 = h\nu_0$$

This expression equates to each other the energy of a photon with frequency ν_0 and energy determined by a certain inertial mass m_0.

Multiple experiments on scattering of **electrons:** Davisson [5, 6], Thomson [7, 8, 9, 10], Biberman [11, 12], Jönsson [13, 14], Pozzi [15, 16, 17], Tonomura [18], ...; **neutrons:** Zeilinger [19], ...; **atoms:** Kanitz [20], ...; **molecules:** Nairz [21], ... aimed at confirming de Broglie's hypothesis showed that, after interacting with a target (slit, wire, polycrystalline film, *etc.*), material particles form on the sensor screen an image of the particle hit intensity distribution which is visually similar to the known diffraction and interference images in optics. As expected, an unambiguous conclusion was made that de Broglie's hypothesis about manifestations of wave properties in material particles is correct, and all doubts should be discarded. This has formed a general attitude of the scientific community towards the problem of impossibility of using the Newtonian mechanics equations for calculating the electron trajectory in the atomic structure [22]. This attitude is also fully characterized by the following quote:

> *There is no need to think that before hitting the emulsion the electron had some trajectory unknown to us. There are no physical indications of its actual existence. Rather, experiments on electron scattering from crystals prove that the motion is fully governed by statistical wave processes, which are completely incompatible with the classical concept of trajectory.*
>
> A.S. Kompaneets [23],p.139

2. Problem definition

The goal of this study is to investigate, within the framework of classical mechanics, the nature and character of electron and neutron scattering from an atomic lattice with accounting for the Coulomb and impact interactions with atomic nuclei. The effect of the moving electron magnetic field on its trajectory in interacting with atomic nuclei is not taken into account, since it will not qualitatively affect the electron scattering pattern but will complicate the calculation of the trajectory within the atomic lattice.

The research consists in solving a number of key problems similar to real experiments[2], namely, electron scattering from two slits, atomic nucleus, polycrystalline structure, and biprism. Neutron scattering and electron reflection from a regular atomic structure are also of significant interest.

The result of each numerical experiment is the distribution of the intensity of particles hitting the sensor screen and its subsequent analysis aimed at realizing what is observed: classical scattering or manifestation of the material particle *wave* properties considered by de Broglie in [1].

3. Model for calculating the particle scattering

3.1. Geometry

Fig. 1 shows the mutual arrangement of components of the calculation scheme for studying material particle scattering from atomic lattices of various types G. The calculation scheme comprises cathode K, diaphragm D, atomic lattice G, two electrically neutral deflectors C and two sensor screens SF and SK. The geometry and structural elements arrangement are specified in the Cartesian frame of reference. Frame-of-reference origin O coincides with the center of cathode K. The lattice G position and orientation is characterized by an additional frame of reference $Ax'y'z'$ coupled with it. Point A is located in the middle of the lattice G lower edge. Vectors $\underline{f}_1, \underline{f}_2, \underline{f}_3$ indicate the direction of the initial flow of single electrons emitted by cathode K and character of its focusing.

A sequence of single electrons e^- with given initial conditions is scattered under interaction with nuclei of atoms constituting lattice G. The use of single electrons eliminates the issue of electron interaction in the beam. Electrons that have overcome an obstacle in the form of lattice G or been reflected from it are recorded by two sensor screens SF and SK, thereby providing

[2]Thomson [7, 8, 9, 10]; Davisson [5, 6]; Biberman [11, 12]; Jönsson [13, 14]; Pozzi [15, 16, 17]; Tonomura [18]; Zeilinger [19]

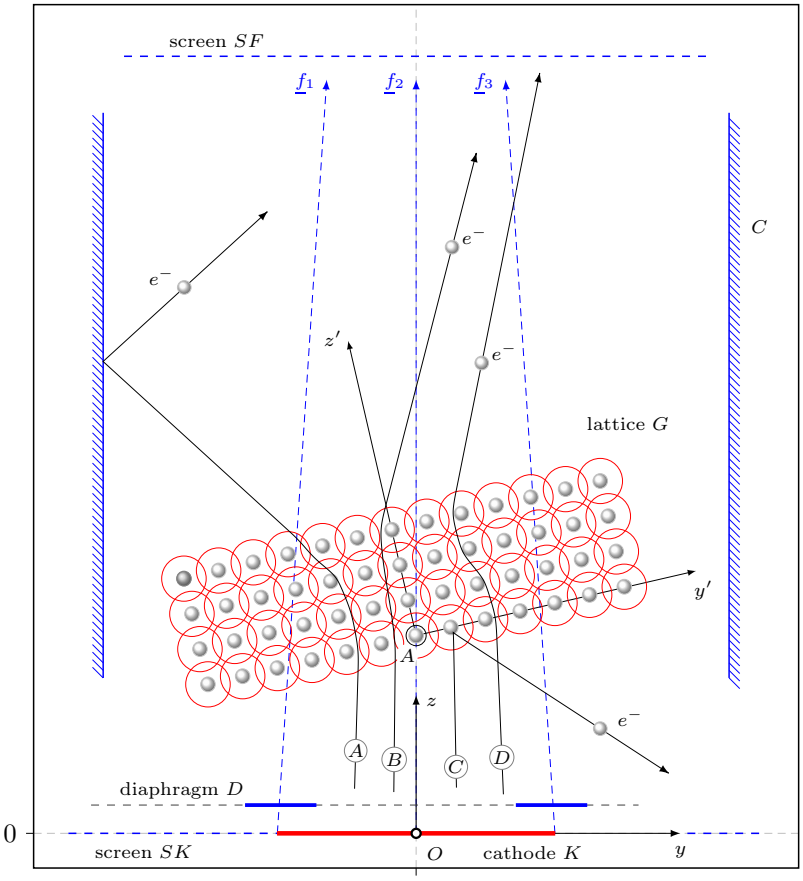

Figure 1. Calculation scheme for examining scattering of material particles from target G. Symbols Ⓐ, Ⓑ, Ⓒ, Ⓓ designate the trajectories of probe electrons.

a distribution of the electron hit intensity along coordinate y represented by relevant curve $I(y)$ and image in the form of a pseudo-photograph.

3.2. Atomic model

Using as an example a gold atom Au, consider a simplified but functional atomic model (Fig. 2). The atom nucleus is considered to be a sphere with radius R_N and charge Q^+ surrounded by a spherical layer, that is, a finite-thickness electron cloud with a uniformly distributed charge equal to Q^- in total and to the nucleus charge in absolute value:

$$Q^- = \sum e^- \,, \quad Q^+ = |Q^-| \,. \tag{2}$$

The outer radius of the electron cloud spherical layer determines atomic radius R_F. Under certain conditions, we may assume that Coulomb charge of the nucleus is completely compensated by the electron cloud charge and

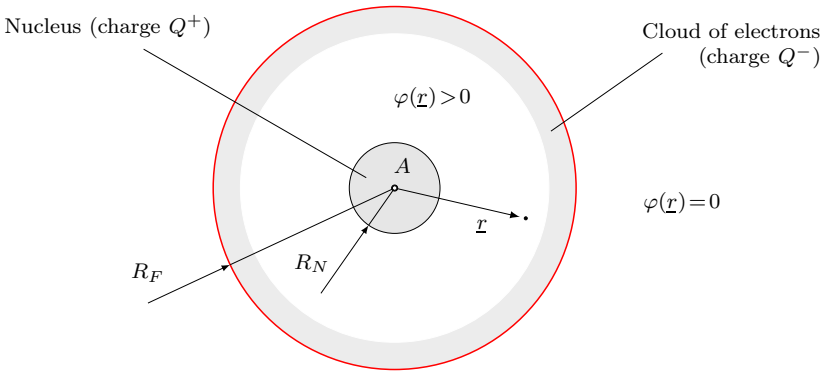

Figure 2. Atomic model

outer electron passing outside the atom does not "feel" its influence until it intersects the surface of sphere having R_F; therefore, assume that total Coulomb potential φ of the nucleus and electron cloud is zero beyond the atom R_F. At the same time, the Coulomb potential inside the atom is determined only by positive nucleus charge Q^+, namely, $\varphi(\underline{r}) > 0$ throughout the entire atom volume. Inside the atom, potential of the spherical layer (electron cloud) is zero.

Making the atomic model more detailed by taking into account the electron cloud structure will technically complicate the task of calculating the outer electron trajectory in the atom's Coulomb field but will not fundamentally change the scattering character. If necessary, we may always represent the electron cloud as a spherical layer with uniformly distributed matter and electric charge and thus take into account its Coulomb potential in calculating the outer electron trajectory inside the atom within the spherical layer.

Actual distribution of electrons hitting the sensor screen is, in general, not only the result of the probabilistic target atom structure but also a combination of such factors as fuzziness of the initial conditions of electron emission from the cathode, inaccuracy in forming its trajectory before and after hitting the target, and also the sensor screen resolution.

Since we are going to account for eccentric collisions of electron or neutron with the atomic nucleus represented as a sphere, let us select an acceptable nucleus radius R_N that allows numerical simulation of the electron — nucleus collision against the background of Coulomb attraction or without it (in the case of a neutron). If for ease of calculation we decide to increase the atomic nucleus physical dimensions, its charge should be appropriately recalculated based on the condition of equality of the electric intensity on the atomic nucleus surface and that on the atomic model nucleus surface:

$$\frac{Q^+}{{R_N^*}^2} = \frac{kQ^+}{{R_N}^2} \quad \Longrightarrow \quad k = \left(\frac{R_N}{R_N^*}\right)^2 . \tag{3}$$

Here k is the scale factor; R_N is the radius of the atomic model nucleus; R_N^* is the real nucleus radius to be calculated via the following empirical formula:

$$R_N^* \approx 1{,}3\sqrt[3]{A} \cdot 10^{-5}\ [\mathring{\text{A}}]\ , \quad A = Z + N\ , \tag{4}$$

where A is the atomic mass number from the Mendeleev's periodic table; Z is the atomic number (the number of protons in the nucleus); N is the number of neutrons in the nucleus. For Au, mass number is $A = 197$, and number of protons is $Z = 79$. Therefore, according to (4), the gold atomic nucleus radius is $R_N^* \approx 7{,}5 \cdot 10^{-5}[\mathring{\text{A}}]$, which is very small compared to the radius of the gold atom Au itself which is $\approx 1{,}44[\mathring{\text{A}}]$.

Thus, introduction in (3) coefficient k at Q^+ allowed accounting for the almost real Coulomb effect on the electron trajectory in approaching the atomic nucleus.

3.3. Particle interaction with atom

The model of scattering of a sequence of single elementary particles, such as electron, positron and neutron, from an obstacle in the form of a regular atomic spatial structure (lattice) includes the following factors: Coulomb interaction with the atomic nucleus, direct physical collision with the nucleus, temperature effects of the atomic lattice.

Basic variants of the effect of positively charged atomic nucleus on the electron, positron and neutron trajectories under relevant initial conditions are shown in Fig. 3.

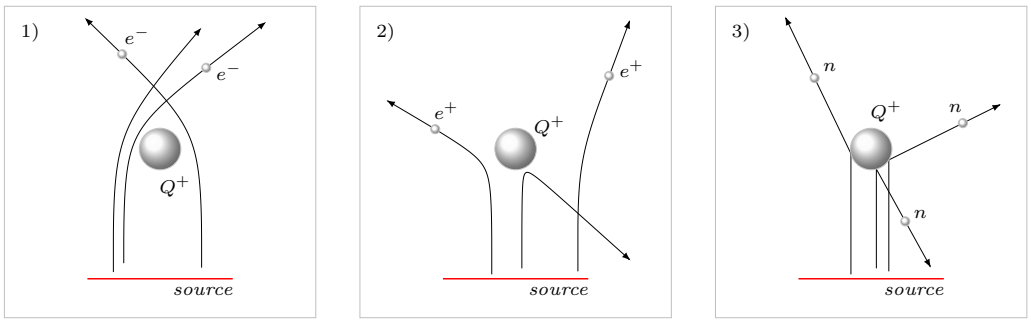

Figure 3. Basic cases of interaction between particles and atomic nucleus. 1) Coulomb attraction of electron e^-; 2) Coulomb repulsion of positron e^+; 3) collision with neutron n.

Collision. Fig. 4 shows a schematic diagram of the collisional interaction between material particle P and atomic nucleus represented by a circle with the center at point A and a radius R_N. Assume that the atomic nucleus

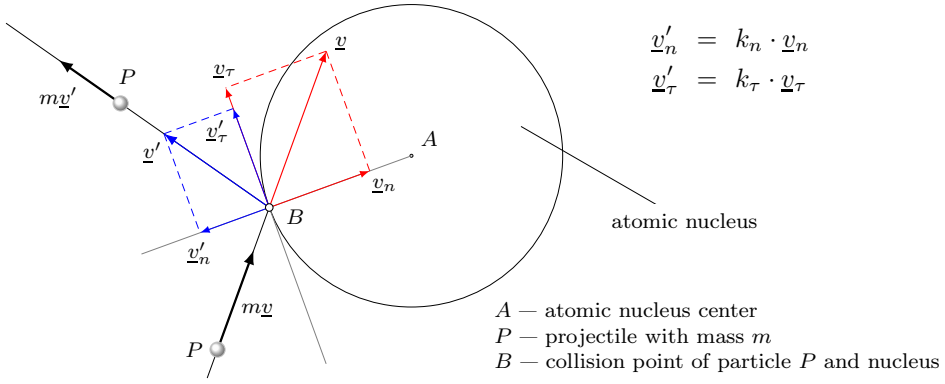

Figure 4. Eccentric collisional interaction of material particle P with atomic nucleus. The collision character is determined by coefficients k_n, k_τ.

remains motionless during its force interaction with an elementary particle, since its inertial mass significantly exceeds that of projectile P. The point of the particle P collision with the nucleus surface is designated by B. Particle P has mechanical momentum $m\underline{v}$. The particle recoil direction (momentum $m\underline{v}'$) is characterized by coefficients k_n, k_τ for the normal and tangential components of velocity $\underline{v}$. In the case of an ideal collision, $k_n = k_\tau = 1$; in general case, $k_n < 1$, $k_\tau < 1$.

3.4. The effect of particle velocity loss

Experiments on accelerating electrons in synchrotrons have shown that the electron moving along a curved trajectory initiates broadband radiation of electromagnetic waves and loses its linear velocity; therefore, this radiation is called bremsstrahlung. In other words, *the electron does work on something or something does work on it.* The same phenomenon is observed also when the electron moves near the atomic nucleus. In this case, the bremsstrahlung impulse duration is determined by duration of the Coulomb interaction between the electron and atomic nucleus. This is where the discreteness of electromagnetic radiation comes from.

To model this physical phenomenon, we introduced into our calculation scheme dissipation coefficient η of a certain conditional medium surrounding the nucleus and atom itself. Coefficient η allows us to naturally reflect the fact that the electron velocity decreases and thus to point out that a part

of its kinetic energy is spent on forming a single bremsstrahlung impulse or plainly an electromagnetic impulse, that is, a photon.

Fig. 5 presents the electron trajectory Ⓒ near the atomic nucleus calculated taking into account dissipation $\eta > 0$; the dashed line represents the trajectory at $\eta = 0$.

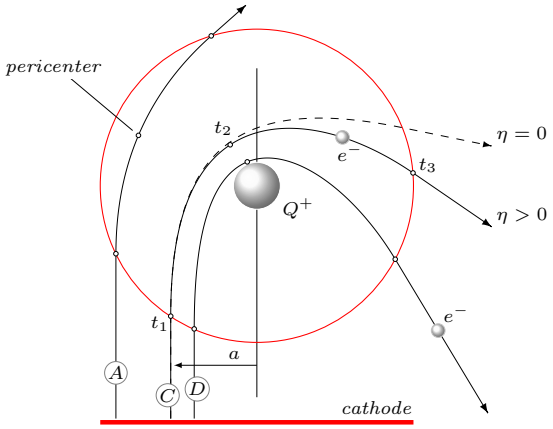

Figure 5. The effect of dissipation parameter η on the electron trajectory near the atomic nucleus. Symbols a is the impact parameter. Ⓐ, Ⓒ, Ⓓ designate the probe electrons and their trajectories.

Having got the area of action of the atomic nucleus Coulomb forces (at time moment t_1), the electron begins losing its velocity, which is accompanied by generation of a broadband bremsstrahlung impulse $\Delta t = t_3 - t_1$ in duration, where t_3 is the moment of leaving the atom's range of influence.

$$|\underline{v}(t)|\Big|_{t=t_1} > |\underline{v}(t)|\Big|_{t=t_3} . \tag{5}$$

Accounting for the dissipation results in an increase in the time of force interaction between the passing-by electron and atomic nucleus, which affects the coordinates of the point of its departure from the atom and its subsequent trajectory.

3.5. Electron motion equation

Within the Newtonian mechanics, let us write a differential equation for determining the electron e^- trajectory among stationary nuclei of the atomic lattice taking into account the Coulomb interaction, collisions, and dissipative medium. The electron may interact with only one or two atoms simultaneously (the case of overlapping between the atoms' areas of action). In the

Cartesian frame of reference $Oxyz$, the dynamic equation for a particle with mass m and charge e^- takes the following form:

$$m\ddot{\underline{r}} = -\frac{1}{4\pi\varepsilon_0}\sum_{i=1}^{N}\delta_i\frac{Q^+e^-}{|\underline{\Delta}_i|^2}\frac{\underline{\Delta}_i}{|\underline{\Delta}_i|} - \eta\,|\underline{v}|^2\frac{\underline{v}}{|\underline{v}|}\,, \qquad \delta_i = \begin{cases} 0\,, & \text{if } \Delta_i > R_F \\ 1\,, & \text{if } \Delta_i \leqslant R_F \end{cases}\,, \quad \text{where} \quad \underline{\Delta}_i = \underline{r}^*_i - \underline{r}\,. \tag{6}$$

Here m, $\underline{r}$ are the electron mass and radius-vector, respectively; N is the number of atoms in the target; Q^+ is the atom nucleus charge; R_F is the atomic radius; e^- is the electron charge; $\underline{r}^*{}_i$ is the radius vector of the i-th atomic nucleus; δ_i is the parameter determining the Coulomb force effect of the i-th atomic nucleus on the electron; $\underline{v} = \dot{\underline{r}}$ is the particle velocity vector; η is the dissipation parameter; ε_0 is the vacuum dielectric constant.

The equation (6) initial conditions are defined as

$$\underline{r}\Big|_{t=0} = \underline{r}_0\,, \quad \dot{\underline{r}}\Big|_{t=0} = \underline{v}_0\,, \tag{7}$$

where $\underline{r}_0$ is the electron radius-vector at the cathode at time moment $t = 0$; $\underline{v}_0$ is the vector of initial velocity of electron emission.

3.6. Accounting for the temperature of atomic lattice

The target temperature as a possible factor affecting the particle trajectory is realized through random independent fluctuations in coordinates of each lattice atom nucleus. Thereat, each emitted electron is scattered from a conditionally "new" obstacle. The temperature effect ($T > 0°K$) visually manifests itself as smearing of intensity of electron hitting the sensor screen cells. Fig. 6 shows how two sequences of single electrons Ⓐ and Ⓑ symmetrical about axis Oz leave blurred traces on sensor screen SF due to random fluctuations in the atomic nucleus coordinates which simulate its temperature $T > 0°K$.

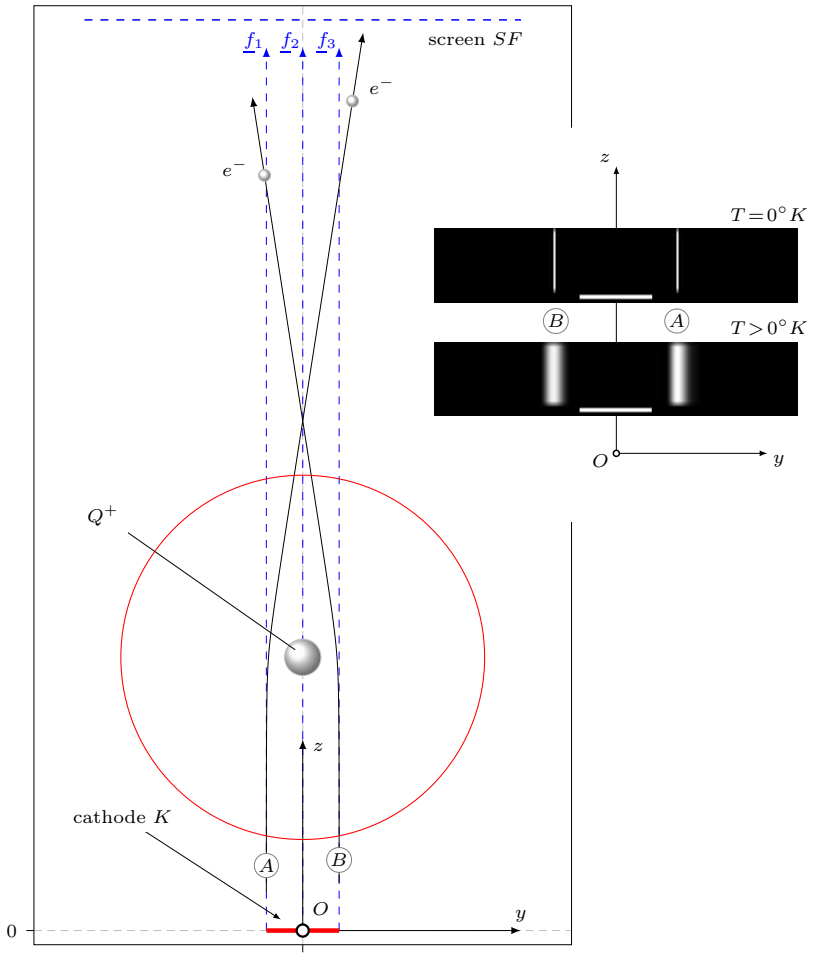

Figure 6. The effect of atomic nucleus temperature in scattering of single electrons from sequences Ⓐ and Ⓑ at the atomic nucleus with charge Q^+.

3.7. Optical component of the calculation model

This part of the model is a conventional optical device, that is, an interferometer consisting of a source of monochromatic electromagnetic radiation and two slits producing an interference pattern on the sensor screen SF with the preset parameters. This interferometer is necessary for analyzing the central part of the particle scattering distribution $I(y)$ in order to reveal the interference. It is known from optics that distribution of the coherent light flux intensity which has passed through an obstacle in the form of several slits is, in general, defined as

$$I^*(y) = I_{const} + I_{max}\left(\frac{\sin u}{u}\right)^2\left(\frac{\sin Nv}{\sin v}\right)^2, \qquad u = \frac{\pi b}{\lambda L}y\,, \quad v = \frac{\pi d}{\lambda L}y\,. \tag{8}$$

Here N is the number of slits; b is the slit width; d is the distance between the slit centers; L is the distance to the screen; λ is the incident wave length; I_{max} is the maximum intensity; I_{const} is the constant component of the intensity.

Consider the case of two slits ($N = 2$); after simplification, relation (8) takes the following form:

$$I^*(y) = I_{const} + 4I_{max}\left(\frac{\sin u}{u}\right)^2 \cos^2 v\,. \tag{9}$$

Expression (9) plays the role an analytical interferometer for constructing interference pattern $I^*(y)$. Interferometer (9) projects the interference $I^*(y)$ pattern onto the sensor screen displaying the electron scattering intensity distribution $I^(y)$. The interferometer (9) parameters at which its interference pattern $I^*(y)$ fits best distributionare $I(y)$ fixed. To estimate the fitting quality, correlation coefficient r is used. This is aimed to visually check the distribution of electron scattering intensity for compliance with the interference pattern.

4. Scattering of elementary particles

A common feature of all the problems is considering particle trajectories in the Oyz plane at the target temperature $T = 0^\circ K$.

4.1. Elementary double-slit obstacle

Fig. 7(p. 13) presents a schematic diagram of the numerical experiment. In the path of a sequence of single electrons emitted by cathode K, target G is placed, which is a one-dimensional lattice of three atoms arranged in one row so as to form two identical gaps simulating two elementary slits. To exclude from consideration the electrons to be reflected towards the cathode, field diaphragm D is used. The result of electron scattering is recorded by sensor screen SF. Central part of the obtained image of the intensity distribution of electrons hitting the screen is well fittable by interference pattern $I^*(y)$ obtained with analytical interferometer (9), which is confirmed by correlation coefficient $r = 0.999$.

4.2. Half-plane

Fig. 8 (p. 14) shows a calculation scheme for considering the influence of the impermeable plate edge on the sequence of ordered electrons emitted by cathode K. As the edge, we consider a single atomic nucleus whose center is located opposite to the cathode K right edge. The result is recorded by sensor screen SF. Intensity distribution $I(y)$ is somewhat similar to the results of

a classical experiment on the monochrome light flux diffraction at the half-plane edge (Fresnel diffraction).

4.3. Regular atomic lattice

Fig. 9 (стр. 15) presents a schematic diagram of the numerical experiment. Target G is placed in the path of single electrons. It is a regular lattice consisting of 7 atomic layers each containing 11 atoms. The atoms partially overlap thus forming areas of joint effect on the electron. The electron scattering is fixed by sensor screen SF. The lattice was overcome by 77% of all the emitted electrons. Central part of the image of the intensity distribution of scattered electrons hitting the screen is well fittable by analytical formula (9), which provides correlation coefficient $r = 0.997$.

4.4. Biprism

Fig. 10 (стр. 16) shows a calculation scheme with a biprism; the biprism is a positively charged nucleus of a single atom which subdivides the electrons emitted by cathode K into two symmetrical fluxes. Here we consider a set of single electrons that are successively emitted with the same initial velocity from initially specified cathode K points.

The results of electron scattering are fixed by sensor screen SF. Expression (9) approximates the central part of obtained intensity distribution $I(y)$ with correlation coefficient $r = 0.999$.

In the framework of the same problem with a biprism, another variant is considered when the biprism wire separating the electron flux is represented in its cross-section as an atomic lattice G inscribed in a circle. This made it possible to consider the nature of electron scattering with accounting for the surface permeability of the wire cross-section atomic structure. The results of simulation are presented in Fig. 11 (p. 17). The sensor screen was reached by 36% of all the emitted electrons. The central part of obtained intensity distribution $I(y)$ correlates well with interference pattern $I^*(y)$ calculated via (9), which is confirmed by correlation coefficient $r = 0.999$.

4.5. Scattering of neutrons

Fig. 12 (стр. 18) shows a calculation scheme for analyzing neutron scattering from an obstacle that partially blocks the cylindrical channel and thereby forms two neutron fluxes. As the obstacle, the atomic nucleus is considered. In general, the calculation scheme matches the real experiment [19]. The results of neutron scattering is displayed on sensor screen SF. In its central part, intensity distribution $I(y)$ fits distribution $I^*(y)$ calculated via (9) with correlation coefficient $r = 0.999$.

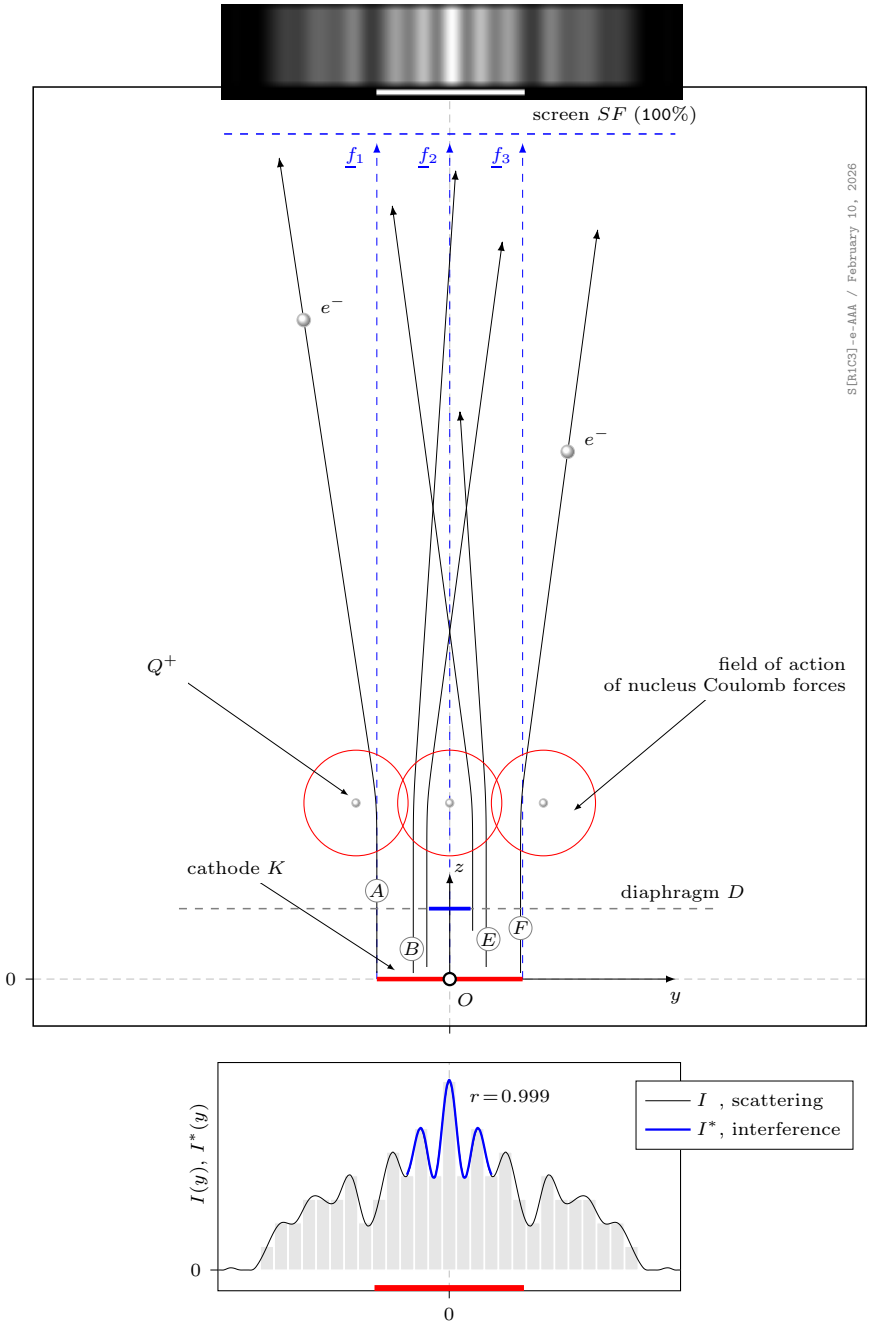

Figure 7. Electron scattering from the elementary double-slit obstacle. Symbols Ⓐ, Ⓑ, Ⓔ, Ⓕ are the probe electron trajectories. The coincidence of distribution $I(y)$ with interference pattern $I^*(y)$ calculated via (9) is shown.

|*See the description in subsection 4.1, p. 11* |

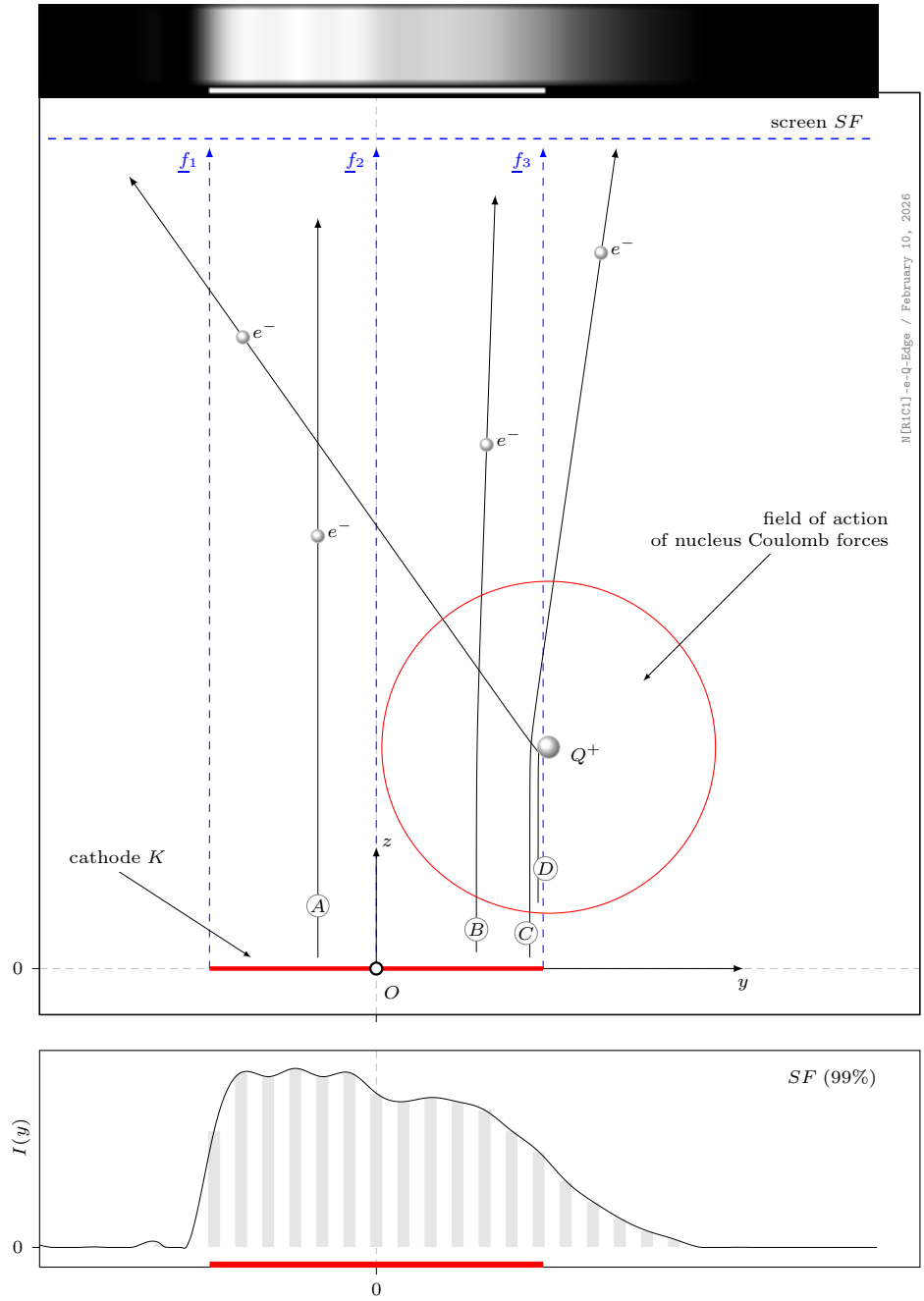

Figure 8. Scattering of a sequence of electrons at the half-plane edge (atomic nucleus). Ⓐ, Ⓑ, Ⓒ, Ⓓ are the probe electron trajectories.
|*See the description in subsection 4.2, p. 11* |

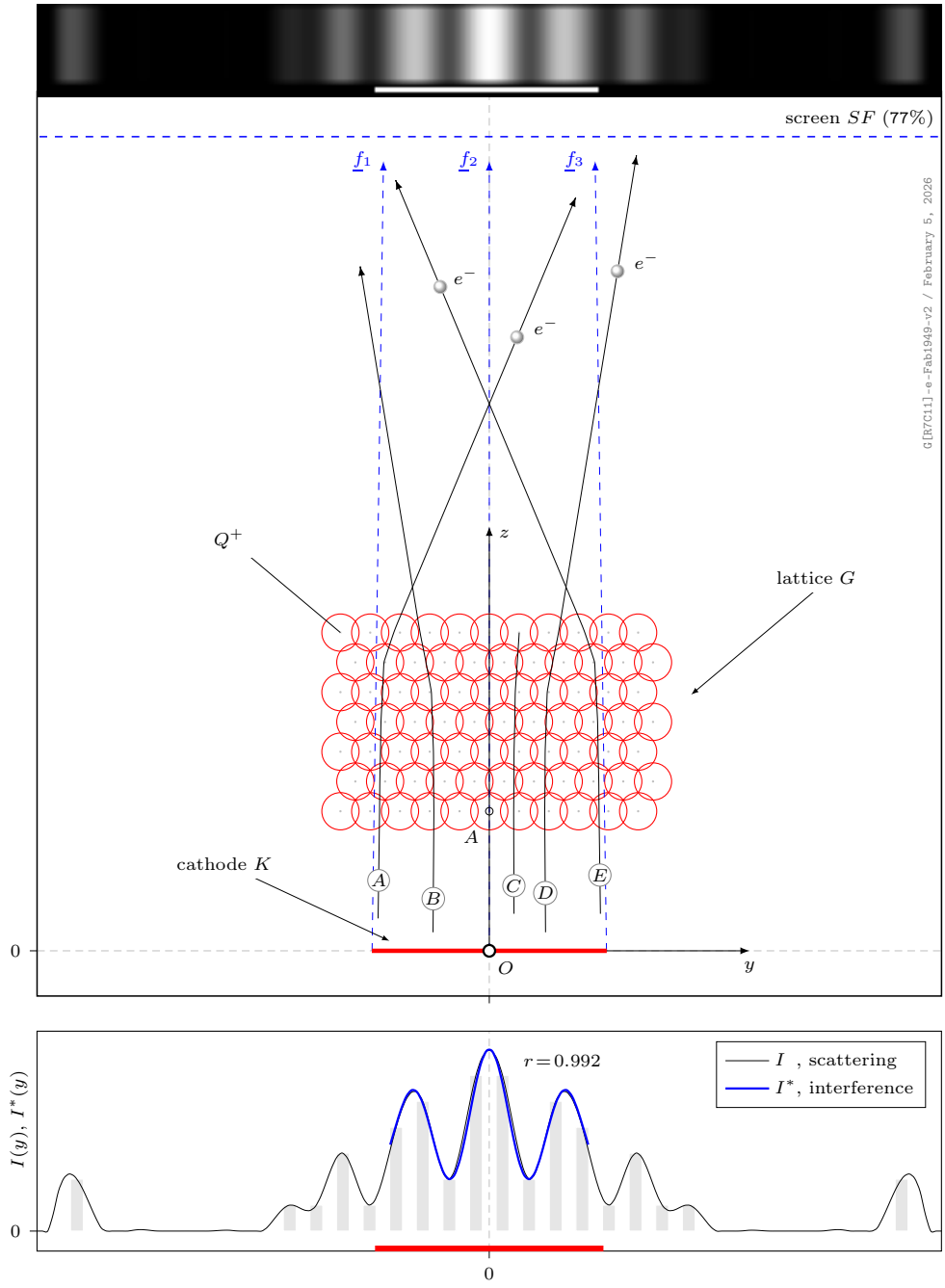

Figure 9. Scattering of single electrons from a regular atomic lattice 7×11. Symbols Ⓐ, Ⓑ, Ⓒ, Ⓓ, Ⓔ are the probe electron trajectories. The coincidence of distribution $I(y)$ with interference pattern $I^*(y)$ calculated via (9) is shown.
|*See the description in subsection 4.3, p. 12* |

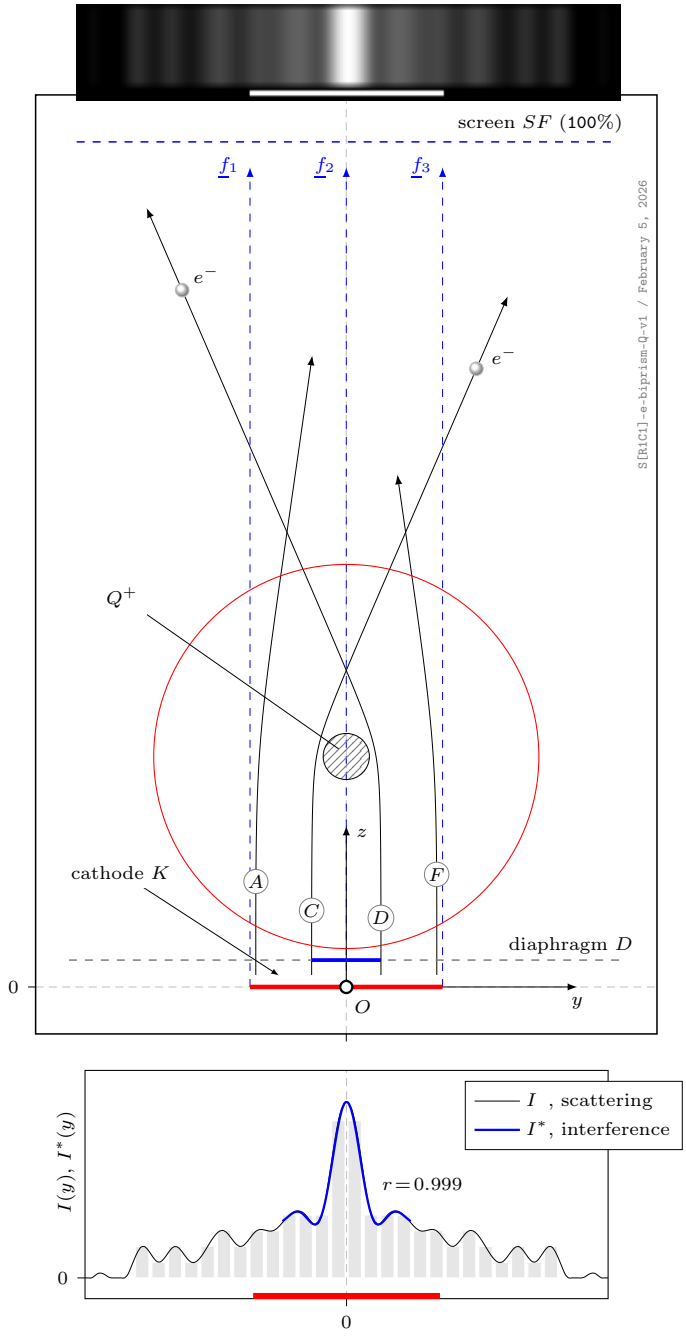

Figure 10. Calculation scheme with a biprism; as the target, an atomic nucleus with charge Q^+ is taken (conventional wire cross-section). Ⓐ, Ⓒ, Ⓓ, Ⓕ are the probe electron trajectories. *See the description in subsection 4.4, p. 12*

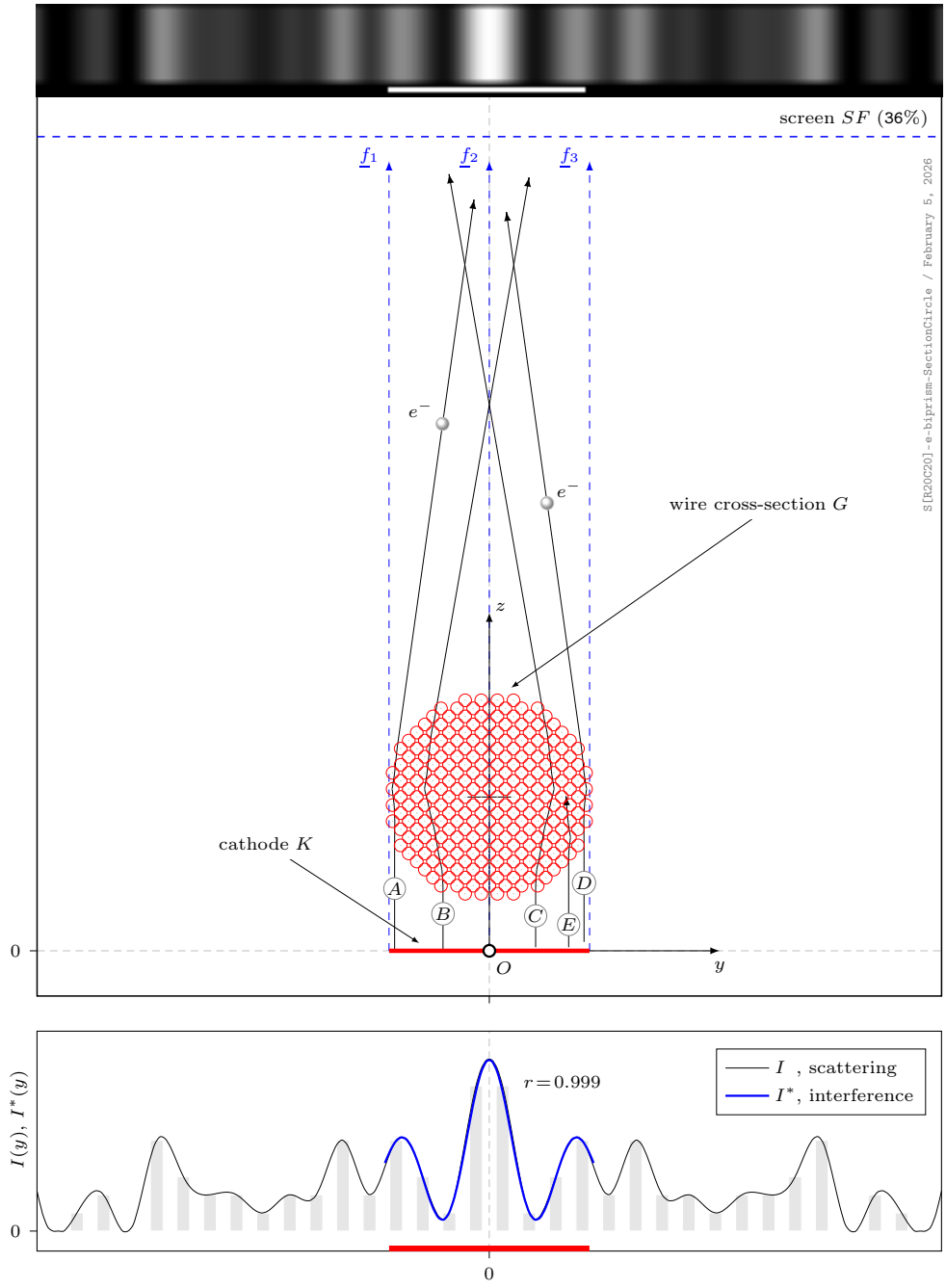

Figure 11. Calculation scheme with a biprism (the target is a wire cross-section, free of external positive potential, in the form of an atomic lattice), which subdivides the electron flux into two ones. 36% of particles have got the screen. Ⓐ, Ⓑ, Ⓒ, Ⓔ, Ⓕ are the probe electron trajectories. |*See the description in subsection 4.4, p. 12* |

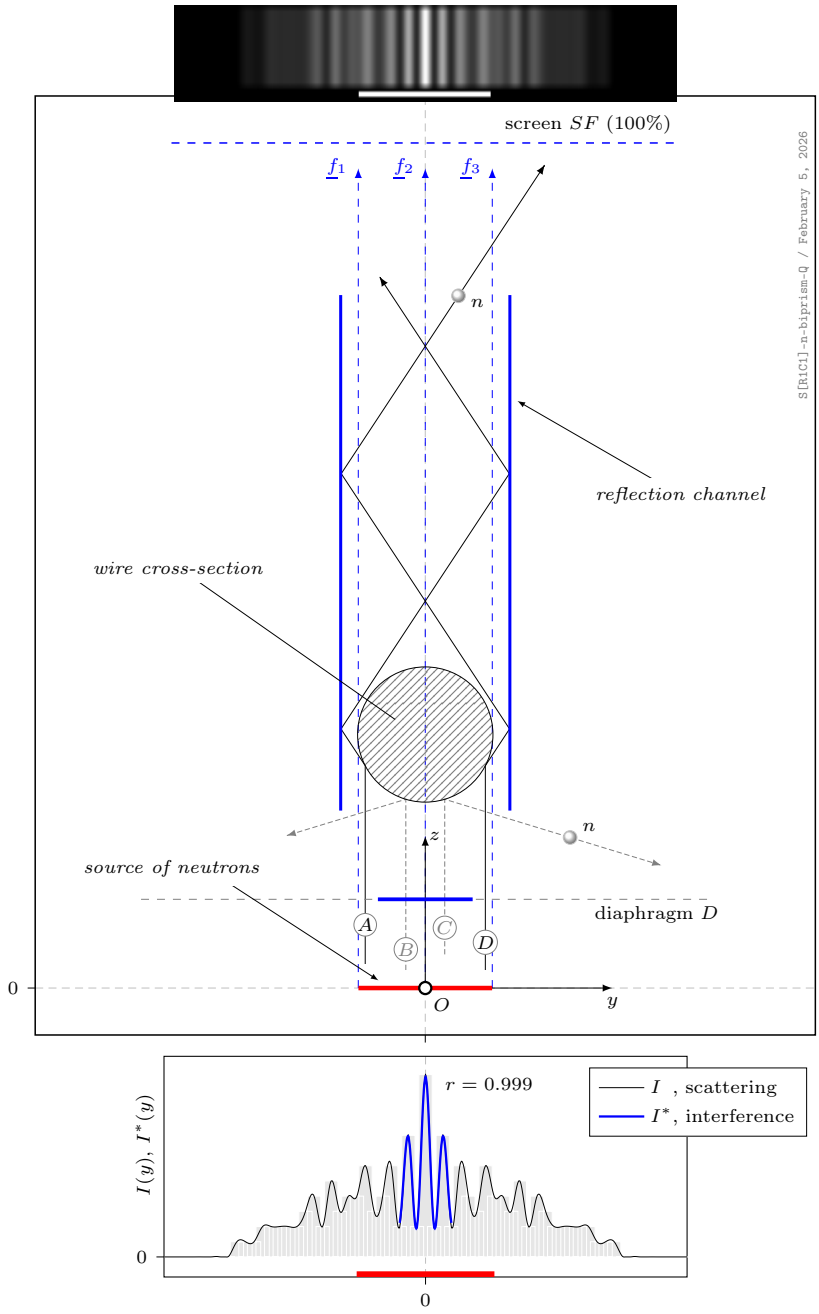

Figure 12. Neutron scattering from the obstacle in the form of a round cross-section (wire). The result of scattering is displayed on sensor screen SF. Symbols Ⓐ, Ⓓ are the probe electron trajectories, while trajectories Ⓑ, Ⓒ are the examples of background trajectories excluded from consideration by field diaphragm D. Central part of the neutron scattering intensity distribution $I(y)$ is fitted by (9).

|*See the description in subsection 4.5, p. 12* |

4.6. Wave interference or particle scattering?

There is no doubt that phenomena such as diffraction and interference are inherent in all wave processes. Is it possible to mistake the intensity distribution of the material particle (electron) scattering from a target obtained in numerous real experiments for diffraction or interference known from classical optical experiments? Similarity in appearance is not yet a basis for an unambiguous conclusion that these material particles have demonstrated their wave properties endowed by de Broglie who, in his turn, relied on the Einstein's hypothesis about the wave-particle duality of the electromagnetic impulse (photon) within which the photon exhibits properties of a material particle with an *inertial mass* dependent on the radiation frequency.

Taking as an example neutron scattering (Fig. 12), consider the calculated intensity distribution of neutrons hitting the sensor screen via analytical interferometer (9). For this purpose, consider the central part of distribution $I(y)$. Let us select the interferometer (9) parameters so as to make interference $I^*(y)$ (blue line) coinciding with distribution $I(y)$. The result is shown in Fig. 12.

The coincidence is almost ideal (with correlation coefficient $r = 0.999$); in other words, optical interference is identical to the neutron distribution over the screen. In our numerical experiment, this fact could be taken as manifestation of the neutron wave properties; however, the calculation model involves only material particles free of any wave properties. Therefore, it is more correct to refer to the calculated over-screen distribution of neutrons $I(y)$ as *pseudo-interference*.

It is known that the interference pattern in experiments with light is the result of spatial superposition of two or more coherent wave processes described by expression (8). Let us check what happens to distributions $I(y)$ and $I^*(y)$ when the sensor screen physical resolution[3] changes by 4 and 16 times with keeping all other problem parameters unchanged, including the settings of analytical interferometer (9). The results are presented in Fig. 13 by three plots.

We can see that, as the sensor screen SF resolution increases, interference pattern $I^*(y)$ calculated via (9) remains unchanged (blue line), while distribution $I(y)$ of neutrons hitting the screen undergoes a significant transformation (black line). At the limit, each particle will occupy only one recording cell of the sensor screen.

Thus, interference $I^*(y)$ of the wave processes (blue line in Fig. 13), as expected, are independent of the sensor screen resolution, which obviously follows just from (8). At the same time, the shape of intensity distribution $I(y)$

[3]The screen physical resolution (`DPI`) is the number of recording cells (pixels) per inch.

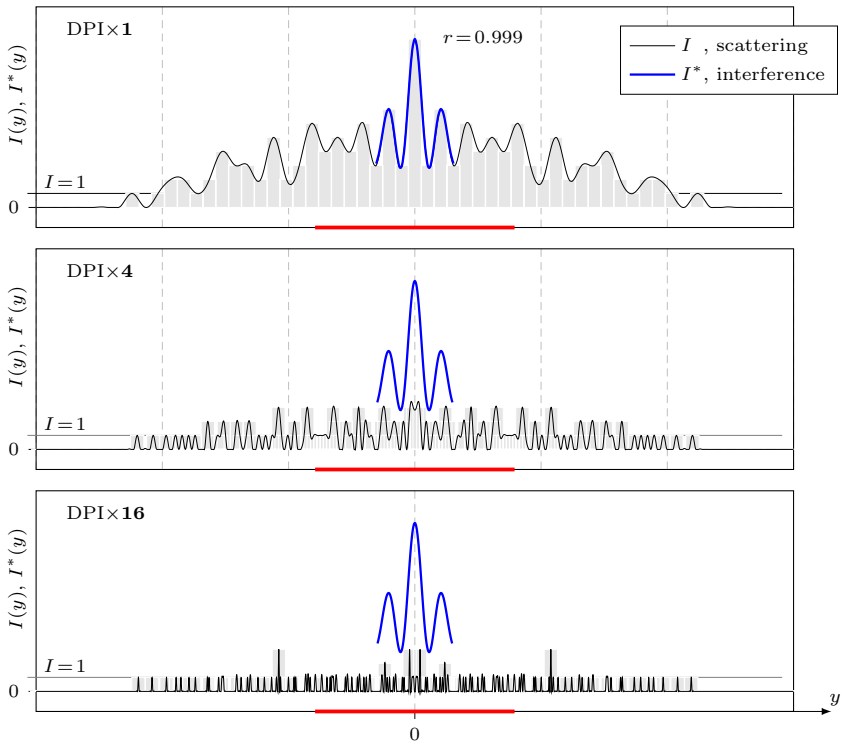

Figure 13. The effect of the sensor screen resolution (factor ×1,×4,×16) on the character of material particle intensity distribution $I(y)$ and interference brought in coincidence with its central part $I^*(y)$.

of neutrons hitting the sensor screen obviously depends on its physical resolution.

Thus, numerical experiments at different sensor screen resolutions (Fig. 13) have shown that neutrons, like other material particles, do not exhibit wave properties at all. The character of particle scattering from the target depends exclusively on initial conditions of emission, external control and parasitic physical fields, fuzzy description of the target structure and temperature, and also on the sensor screen resolution and sensitivity.

Note the duality of the sensor screen: in the case of wave processes, it displays the spatial *superposition* of waves but does not participate in their summation, while in the case of material particle scattering the sensor screen *sums* (accumulates) the particles. Thus, the sensor screen functional role, that is, to display or to summarize, is determined by the problem definition.

The final point in interpreting the nature of neutron or electron scattering from the target atomic structure may be put by ***experimentum crucis***[4].

[4]In Latin this means "crucial experiment".
The term was introduced by *Francis Bacon* (1561–1626).

which means conducting a series of particle-scattering experiments at different sensor-screen resolutions.

5. Reflection of electrons

Consider the process of reflection of a sequence of single electrons from a target surface represented by a layer of equidistant atoms. The operating configuration of the model is shown in Fig. 14.

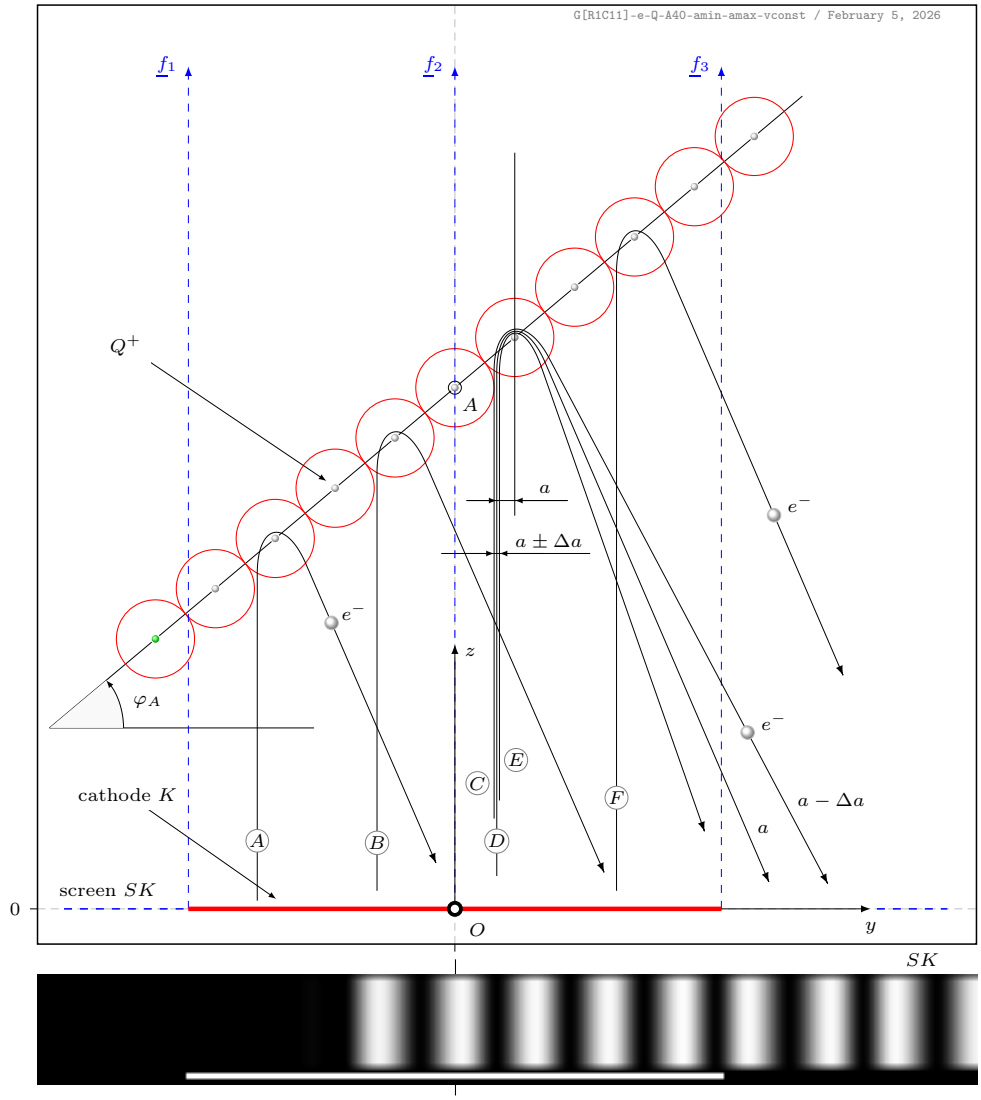

Figure 14. Electron reflection from a surface in the form of a regular atomic structure. Symbol a is the impact parameter.

The effect of reflection is based on the Coulomb interaction of electrons with nuclei of the lattice atoms. How do electrons behave when they hit the target "surface" oriented at angle φ_A to the screen SK plane? Some of the electrons undergo reflection while going around the atomic nucleus being accompanied by bremsstrahlung (similar to the processes taking place in an x-ray tube); remaining electrons form the background, that is, randomly reflect without a predominant direction and scatter throughout the volume of the target's atomic lattice.

To examine the mechanism of electron reflection from the target surface, we selected among all the electrons emitted by cathode K only those which orderly reflect in interacting with atomic nuclei and form on the sensor screen a series of equidistant bands whose shape is fully determined by initial conditions of electron emission from cathode K and parameters of atomic lattice G.

6. Conclusions

Pseudo-interference. The type of intensity distribution of material particles hitting the sensor screen in experiments with **electrons:** Davisson [5, 6], Thomson [7, 8, 9, 10], Biberman [11, 12], Jönsson [13, 14], Pozzi [15, 16, 17], Tonomura [18], ...; **neutrons:** Zeilinger [19], ...; **atoms:** Kanitz [20], ...; **molecules:** Nairz [21], ... are, in essence, neither diffraction nor interference. In actual fact, only ordinary scattering of material particles (pseudo-interference) was detected in the experiments as a result of particle collisions and Coulomb interaction with nuclei of target atoms.

The question of what the sensor screen records, either the interference pattern or scattering of material particles, may be answered only in one objective way, namely, by conducting an ***experimentum crucis*** at different sensor screen resolutions.

It is evident that the interference pattern of wave processes does not change with varying sensor screen resolution. One the other hand, in the case of material particles, the increase in the screen resolution (`DPI`) induces an increase in the scattering field detailing and equalization of the intensity distribution $I(y)$ amplitude (Fig. 13) reflected on the sensor screen; at the limit, the amplitude tends to unity, i.e. one hit per sensor screen recording cell.

For more detailed justification of why the de Broglie's hypothesis about the material particle wave properties is unacceptable, we should address such a phenomenon as wave-particle duality postulated by Einstein.

Wave-particle duality. We mean by term "photon" a single electromagnetic impulse resulting from bremsstrahlung of an electron, proton or other particle moving along a curved trajectory. It is commonly believed that a photon has inertial mass while moving with the velocity of light, while its mass at rest is zero. Here an obvious question arises: what is the photon's inertial mass?

The concept of photon mass appeared in Einstein's works on the photoelectric effect [3] where he established a relationship between the electromagnetic radiation energy and electron emission from the photocathode. To explain the photoelectric effect, Einstein injected the idea of the corpuscular nature of photons; he represented them as material particles having inertial mass when moving at the velocity of light. This was used as a methodological technique to overcome the problem of how an immaterial photon (electromagnetic impulse) performs work on a material electron in photocathode.

Thus, the Einstein's hypothesis of wave-particle duality implies that an electromagnetic impulse (photon) has inertial mass while moving at the velocity of light. However, this contradicts the special theory of relativity in which Einstein postulated that no material body with inertial mass can reach the velocity of light. Moreover, in order to introduce the concept of mass of something material, it is first necessary to define the physical volume confining this material object. But what volume can we talk about in the case of electromagnetic impulse (photon)?

Electromagnetic impulse (photon) fundamentally cannot have a physical volume by its nature, and, therefore, cannot have inertial mass at all; hence, it cannot also have mechanical momentum (the product of mass and velocity).

Therefore, the fact that the photon has no volume needs recognizing that it is not a particle with mass but merely a massless electromagnetic impulse with its own amplitude, duration and frequency. One question remains open: how does a massless electromagnetic impulse transfer its energy to an electron having inertial mass in photocathode experiments? A material object to be used as a "foothold" is needed. Probably, it is necessary to put into consideration a *material medium* where electromagnetic oscillations (photons) propagate and which is able to transmit a mechanical impulse to material particles.

On the Louis de Broglie's hypothesis. Let us return to the de Broglie's hypothesis about wave properties of material particles. The de Broglie's assumption is quaint but untenable from the very beginning, since his reasoning relied on the hypothesis of the photon's corpuscular-wave duality suggested by Einstein; however, as shown above, the photon is not a corpuscle with

inertial mass but merely a massless electromagnetic impulse and, therefore, there are no reasons for attributing wave properties to material particles.

In its classical sense, interference between two material particles is impossible since they do not have a wave front and actually cannot be at the same time at the same spatial point. Assume hypothetically that we succeeded in creating coherence conditions for the emitted particles; then these particles would physically collide at a point on the device optical axis and change their trajectories, which is absolutely unnatural for wave processes.

* * *

The performed numerical experiments have shown that pseudo-interference observed in real experiments on scattering of electrons and other material particles does not require imparting to the particles properties inherent exclusively to wave processes.

Discreteness of natural electromagnetic oscillations is physically determined by the discreteness of bremsstrahlung sources. A photon as an electromagnetic pulse of the bremsstrahlung origin cannot be a particle having the inertial mass and at the same time having no physical volume that is absolutely necessary for defining the mass concept itself and, hence, mechanical momentum (certainly, in the framework of classical mechanics). Thus, there are no reasons to accept the phenomenon of corpuscular-wave duality and de Broglie wave concept.

Pseudo-interference of material particles observed in numerical and real experiments during scattering from an obstacle has no concern to the particles' wave properties because of their total absence. This may be clearly demonstrated in the ***experimentum crucis*** when the type of scattered-particle intensity distribution is considered on the sensor screen at different resolutions.

References

[1] L. V. P. R. de Broglie, "Ondes et quanta," *C. R. Acad. Sci. Paris*, vol. 177, p. 507, 1923.

[2] L. de Broglie, *La physique nouvelle et les quanta.* Bibliothèque de philosophie scientifique, Flammarion, 1937.

[3] A. Einstein, "Über einen die Erzeugung und Verwandlung des Lichtes betreffenden heuristischen Gesichtspunkt," *Annalen der Physik*, vol. 322, pp. 132–148, jan 1905.

[4] H. Mark and R. Wierl, *Diffraction of electrons*. Moscow: GTTI, 1933.

[5] C. Davisson and L. H. Germer, "The scattering of electrons by a single crystal of nickel," *Nature*, vol. 119, pp. 558–560, Apr 1927.

[6] C. Davisson and L. H. Germer, "Diffraction of electrons by a crystal of nickel," *Phys. Rev.*, vol. 30, pp. 705–740, Dec 1927.

[7] G. P. Thomson and A. Reid, "Diffraction of Cathode Rays by a Thin Film," *Nature*, vol. 119, pp. 890–890, June 1927.

[8] G. P. Thomson, "Experiments on the Diffraction of Cathode Rays," *Proceedings of the Royal Society of London Series A*, vol. 117, pp. 600–609, Feb. 1928.

[9] G. P. Thomson, "Experiments on the Diffraction of Cathode Rays. II," *Proceedings of the Royal Society of London Series A*, vol. 119, pp. 651–663, July 1928.

[10] G. P. Thomson, "Diffraction of Cathode Rays. III," *Proceedings of the Royal Society of London Series A*, vol. 125, pp. 352–370, Sept. 1929.

[11] L. Biberman, N. Sushkin, and V. Fabrikant, "Diffraction of electrons moving in succession," *Doklady Akad. Nauk S.S.S.R.*, vol. LXVI, pp. 185–186, 01 1949.

[12] L. Biberman, E. Vtorov, I. Kovner, and N. Sushkin, "Scattering of electrons in thin layers," *Doklady Akad. Nauk S.S.S.R.*, vol. LXIX, no. 4, pp. 519–520, 1949.

[13] C. Jönsson, "Elektroneninterferenzen an mehreren künstlich hergestellten Feinspalten," *Zeitschrift fur Physik*, vol. 161, pp. 454–474, Aug. 1961.

[14] C. Jönsson, "Electron Diffraction at Multiple Slits," *American Journal of Physics*, vol. 42, pp. 4–11, Jan. 1974.

[15] O. Donati, G. P. Missiroli, and G. Pozzi, "An Experiment on Electron Interference," *American Journal of Physics*, vol. 41, pp. 639–644, May 1973.

[16] G. Matteucci, G. Missiroli, G. Pozzi, P. Merli, and I. Vecchi, "Interference electron microscopy in thin film investigations," *Thin Solid Films*, vol. 62, pp. 5–17, Sept. 1979.

[17] S. Frabboni, G. C. Gazzadi, and G. Pozzi, "Young's double-slit interference experiment with electrons," *American Journal of Physics*, vol. 75, pp. 1053–1055, Nov. 2007.

[18] A. Tonomura, J. Endo, T. Matsuda, T. Kawasaki, and H. Ezawa, "Demonstration of single-electron buildup of an interference pattern," *American Journal of Physics*, vol. 57, pp. 117–120, Feb. 1989.

[19] A. Zeilinger, R. Gähler, C. G. Shull, W. Treimer, and W. Mampe, "Single- and double-slit diffraction of neutrons," *Rev. Mod. Phys.*, vol. 60, pp. 1067–1073, Oct. 1988.

[20] C. Kanitz, J. Bühler, V. Zobač, J. J. Robinson, T. Susi, M. Debiossac, and C. Brand, "Diffraction of atomic matter waves through a 2d crystal," 2024.

[21] O. Nairz, M. Arndt, and A. Zeilinger, "Quantum interference experiments with large molecules," *American Journal of Physics*, vol. 71, pp. 319–325, Apr. 2003.

[22] P. Davies, *Superforce*. A Touchstone book, Touchstone, 1985.

[23] A. Kompaneets, *Symmetry in the micro- and macrocosm*. NAUKA, 1978.